

S & M 0763

# Microstructural Control of Mesoporous SnO<sub>2</sub> Powders and Their H<sub>2</sub> Sensing Properties

Naoyuki Hario, Takeo Hyodo, Yasuhiro Shimizu<sup>1,\*</sup> and Makoto Egashira<sup>1</sup>

Graduate School of Science and Technology, Nagasaki University  
<sup>1</sup>Department of Materials Science and Engineering, Faculty of Engineering,  
Nagasaki University 1-14 Bunkyo-machi, Nagasaki 852-8521, Japan

(Received March 9, 2009; accepted May 11, 2009)

**Key words:** tin dioxide, mesoporous structure, agglomerate, ultrasonic treatment, H<sub>2</sub> sensor

Several approaches have been tested to reduce the size of mesoporous tin oxide (m-SnO<sub>2</sub>) agglomerates prepared by utilizing the self-assembly of *n*-cetylpyridinium chloride. The variables and methods tested were the mixing ratio of Na<sub>2</sub>SnO<sub>3</sub>·3H<sub>2</sub>O as a tin source and trimethylbenzene in the precursor solution, stirring or ultrasonic treatment after the hydrolysis of the precursor solution, and mechanical grinding of resulting m-SnO<sub>2</sub> powders in an agate motor. Among them, ultrasonic treatment immediately after the hydrolysis of Na<sub>2</sub>SnO<sub>3</sub>·3H<sub>2</sub>O was very effective in reducing agglomerate size and in obtaining a large specific surface area (SSA) of more than 300 m<sup>2</sup> g<sup>-1</sup>, even after calcination at 600°C for 5 h, while grinding in the agate mortar after the calcination led to a decrease in SSA of all m-SnO<sub>2</sub> powders. The m-SnO<sub>2</sub> sensor fabricated with ultrasonically treated powder showed relatively high H<sub>2</sub> sensing properties, probably owing to the small-size agglomerates and large SSA.

## 1. Introduction

Semiconductor-type gas sensors, which were first proposed by Seiyama *et al.* in 1962,<sup>(1)</sup> can detect a wide variety of gases, *e.g.*, H<sub>2</sub>, NO<sub>x</sub>, CO and volatile organic compounds (VOCs), by utilizing a difference in the electrical resistance of semiconductor metal oxides between a base gas and a test gas.<sup>(2)</sup> Among various sensor materials, SnO<sub>2</sub> is an ideal and important material for semiconductor-type gas sensors.<sup>(3)</sup> Therefore, various types of nanostructured SnO<sub>2</sub> such as nanoparticles,<sup>(4)</sup> nanowires,<sup>(4,6,7)</sup> nanobelts<sup>(4)</sup> and nanorods<sup>(4,8)</sup> have been prepared as gas-sensor materials by a general sol-gel technique,<sup>(9,10)</sup> a hydrothermal or solvothermal method,<sup>(9)</sup> or some physical vapor deposition methods<sup>(11,12)</sup> because they have provided a promising way towards miniaturized ultrasensitive gas sensors.<sup>(9)</sup> Recently, mesoporous SnO<sub>2</sub> (m-SnO<sub>2</sub>) powder has also been prepared by employing the self-assembly of *n*-cetylpyridinium chloride as a template and Na<sub>2</sub>SnO<sub>3</sub> as a tin source, and thermal stabilizing by a treatment in an

---

\*Corresponding author: e-mail: shimizu@nagasaki-u.ac.jp

aqueous phosphoric acid solution.<sup>(13,14)</sup> The thermally stable m-SnO<sub>2</sub> obtained showed an extremely large specific surface area (SSA > 300 m<sup>2</sup> g<sup>-1</sup>, even after calcination at 600°C), but the sensor responses to H<sub>2</sub> and NO<sub>x</sub> were smaller than expected, probably owing to the large agglomerate size of the m-SnO<sub>2</sub> powder.<sup>(14)</sup> Large m-SnO<sub>2</sub> agglomerates were considered to grow during the hydrolysis of a tin source and the subsequent aging process in the aqueous solution.

In this study, therefore, reduction of m-SnO<sub>2</sub> agglomerate size has been attempted by controlling the preparation conditions, by ultrasonic or stirring treatment of the precursor solution, and by mechanical grinding of resultant agglomerates. The effects of these treatments on the gas sensing properties of the m-SnO<sub>2</sub> sensors fabricated with different powders using 1000 ppm H<sub>2</sub> in air as the test gas were examined.

## 2. Materials and Methods

### 2.1 Synthesis of m-SnO<sub>2</sub> powders

m-SnO<sub>2</sub> powders were prepared from precursor solutions of mixtures of *n*-cetylpyridinium chloride (C<sub>16</sub>PyCl) as a template, Na<sub>2</sub>SnO<sub>3</sub>·3H<sub>2</sub>O (SS) as a tin source, and trimethylbenzene (mesitylene: MES) as an additive. The typical preparation procedure was as follows. C<sub>16</sub>PyCl was added to deionized water at 2.0 wt%, and an aqueous solution of 0.027 mol dm<sup>-3</sup> Na<sub>2</sub>SnO<sub>3</sub> was mixed with the aqueous C<sub>16</sub>PyCl solution at a molar ratio of [C<sub>16</sub>PyCl]/[SS] = 2.0. To investigate the effect of MES addition on mesoporous structure, MES was also added to the mixed solution at molar ratios of [MES]/[SS] = 0, 1.0, 2.0 and 2.5. The pH of the solution was then adjusted to approximately 10 with an aqueous 35 wt% HCl solution. A solid product formed at the bottom of the reactor immediately after the pH adjustment. The resultant solid product was allowed to stand for 12 h in the solution at 20°C for aging. In some cases, the precursor solution was treated ultrasonically for 10 min with an ultrasonic homogenizer (Nihon Seiki, G1081-4, 19.5 kHz) immediately after the pH adjustment or stirred mechanically during the entire aging period. After the aging, the resultant solid product was filtered off and washed with deionized water. Thereafter, the resultant solid was immersed in an aqueous solution of approximately 33 mM phosphoric acid for 2 h, and then it was filtered off, washed and dried at 80°C overnight. The preparation conditions of various m-SnO<sub>2</sub> powders are listed in Table 1. Finally, the powders were calcined at 600°C for 5 h in air. In some cases, the calcined powder was subjected to mechanical grinding. Hereafter, the powders will be referred to by their sample numbers listed in Table 1. The morphology of the porous SnO<sub>2</sub> powders obtained was observed by scanning electron microscopy (SEM, Hitachi, S2250-N).

### 2.2 Fabrication of m-SnO<sub>2</sub> sensors and their hydrogen sensing properties

Thick film sensors were fabricated by screen-printing m-SnO<sub>2</sub> pastes on an alumina substrate equipped with a pair of interdigitated Pt electrodes, followed by calcination at 550°C for 5 h in air. Again the sensors will be referred to by the sample numbers

Table 1  
Preparation conditions of various m-SnO<sub>2</sub> powders.

Sample No.	[MES]/[SS*] (molar ratio)	UT**	Stirring during aging	MG***
0M	0	No	No	No
0M-G	0	No	No	Yes
1.0M	1.0	No	No	No
1.0M-G	1.0	No	No	Yes
2.0M	2.0	No	No	No
2.0M-G	2.0	No	No	Yes
2.5M	2.5	No	No	No
2.5M-G	2.5	No	No	Yes
2.5M-S	2.5	No	Yes	No
2.5M-S-G	2.5	No	Yes	Yes
2.5M-U	2.5	Yes	No	No
2.5M-U-G	2.5	Yes	No	Yes

\*SS: Na<sub>2</sub>SnO<sub>3</sub>·3H<sub>2</sub>O, \*\*UT: ultrasonic treatment, \*\*\*MG: mechanical grinding.

listed in Table 1. Gas responses of these sensors to 1000 ppm H<sub>2</sub> balanced with air were measured in a flow apparatus at 250–500°C. The sensor response was defined as the ratio ( $R_a/R_g$ ) of sensor resistance in air ( $R_a$ ) to that in H<sub>2</sub> balanced with air ( $R_g$ ).

### 3. Results and Discussion

#### 3.1 Effect of amount of MES added

Figures 1 and 2 show SEM photographs and pore size distributions of m-SnO<sub>2</sub> powders prepared at various molar ratios of MES/SS. These powders were not subjected to ultrasonic treatment (UT) or mechanical grinding (MG). Low-resolution SEM photographs showed that all the m-SnO<sub>2</sub> powders consisted of extremely large agglomerates (250–430 μm in diameter), regardless of the amount of MES added. On the other hand, it was confirmed from the high-resolution SEM photographs that these large agglomerates consisted of fine m-SnO<sub>2</sub> particles of about 1.7–5.7 μm in diameter. Such morphology suggests that the macroscopic m-SnO<sub>2</sub> particles were formed by agglomeration of fine m-SnO<sub>2</sub> particles and that the size of the agglomerates could not be controlled at all by adjusting the amount of MES added to the precursor solution. As expected from our previous studies,<sup>(12,13)</sup> all the powders had a large pore volume at a pore diameter of about 1.6–2.0 nm with an SSA larger than 300 m<sup>2</sup> g<sup>-1</sup>, as shown in Fig. 2. Thus, we can confirm that the mesoporous structure was well developed already in the fine SnO<sub>2</sub> particles.

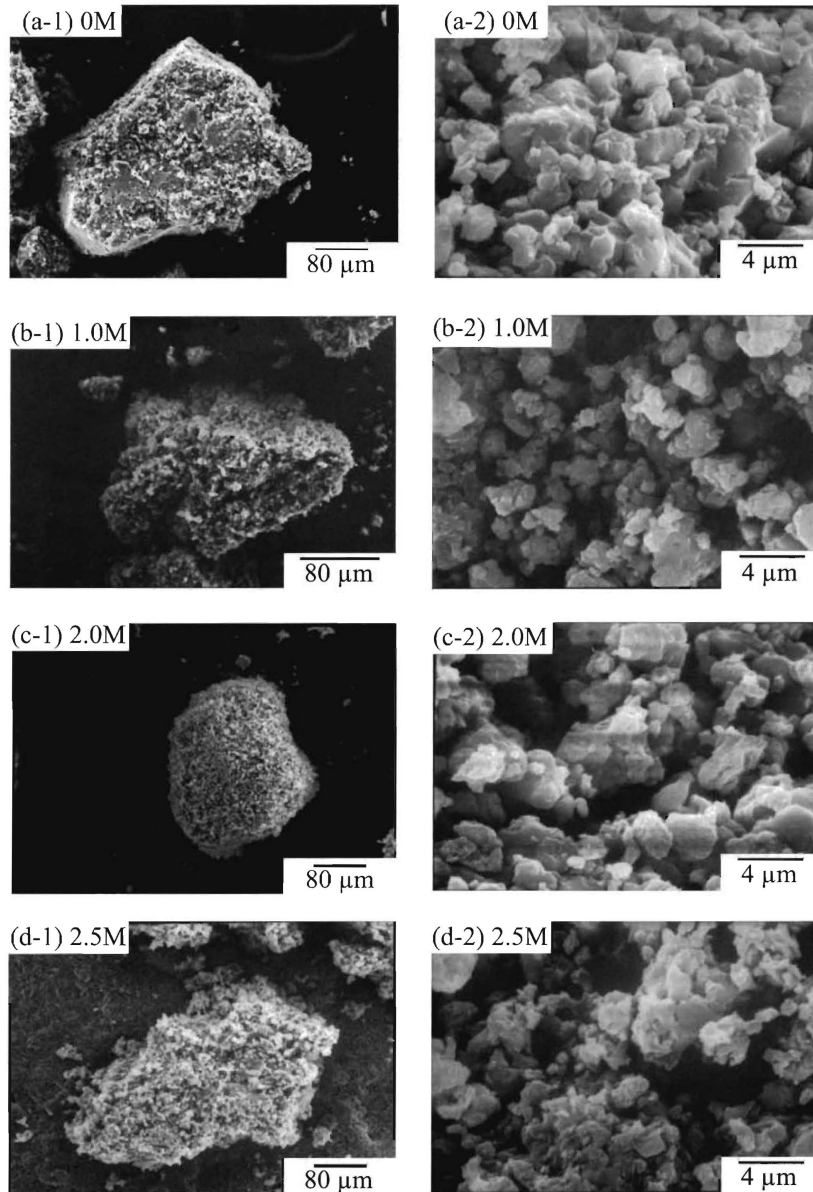


Fig. 1. SEM photographs of  $m\text{-SnO}_2$  powders prepared at various molar ratios of MES/SS. The powders were not subjected to UT or MG.

The powders shown in Fig. 1 were then subjected to MG. After MG, it is obvious that the size of all  $m\text{-SnO}_2$  agglomerates was largely reduced to less than 10 μm in diameter, as shown in Fig. 3, indicating a very brittle nature of these agglomerates. On the other hand, from comparison between the high-resolution SEM photographs shown in Figs. 1 and 3, it was revealed that the size of fine  $m\text{-SnO}_2$  particles generally



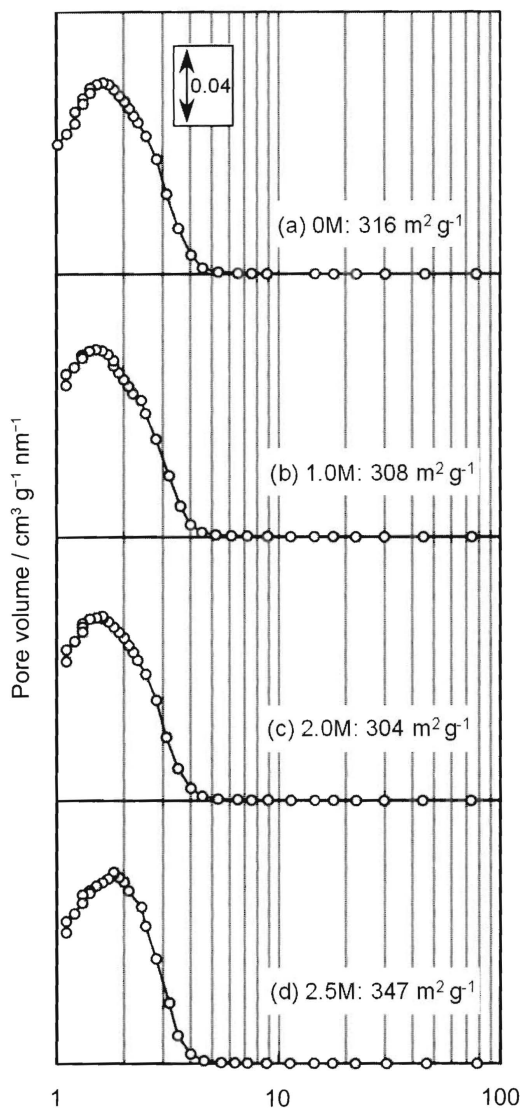


Fig. 2. Pore size distributions of  $m\text{-SnO}_2$  powders prepared at various molar ratios of MES/SS. The powders were not subjected to UT or MG.

remained almost unchanged following MG. However, many  $\text{SnO}_2$  nanoparticles of less than 500 nm in diameter, which were probably the particles that fractured during MG, were observed on the surface of fine particles of micron size. Figure 4 shows the pore size distributions of these ground powders and their SSAs. The pore size distribution was hardly changed by MG for all the powders, but the pore volume at a pore diameter of about 2.0 nm and SSA decreased markedly after MG. Thus, part of the mesoporous structure was collapsed by MG and the collapse percentages were calculated to be 29.4, 24.0, 24.4 and 28.8% for the 0, 1.0, 2.0 and 2.5 M powders, respectively.

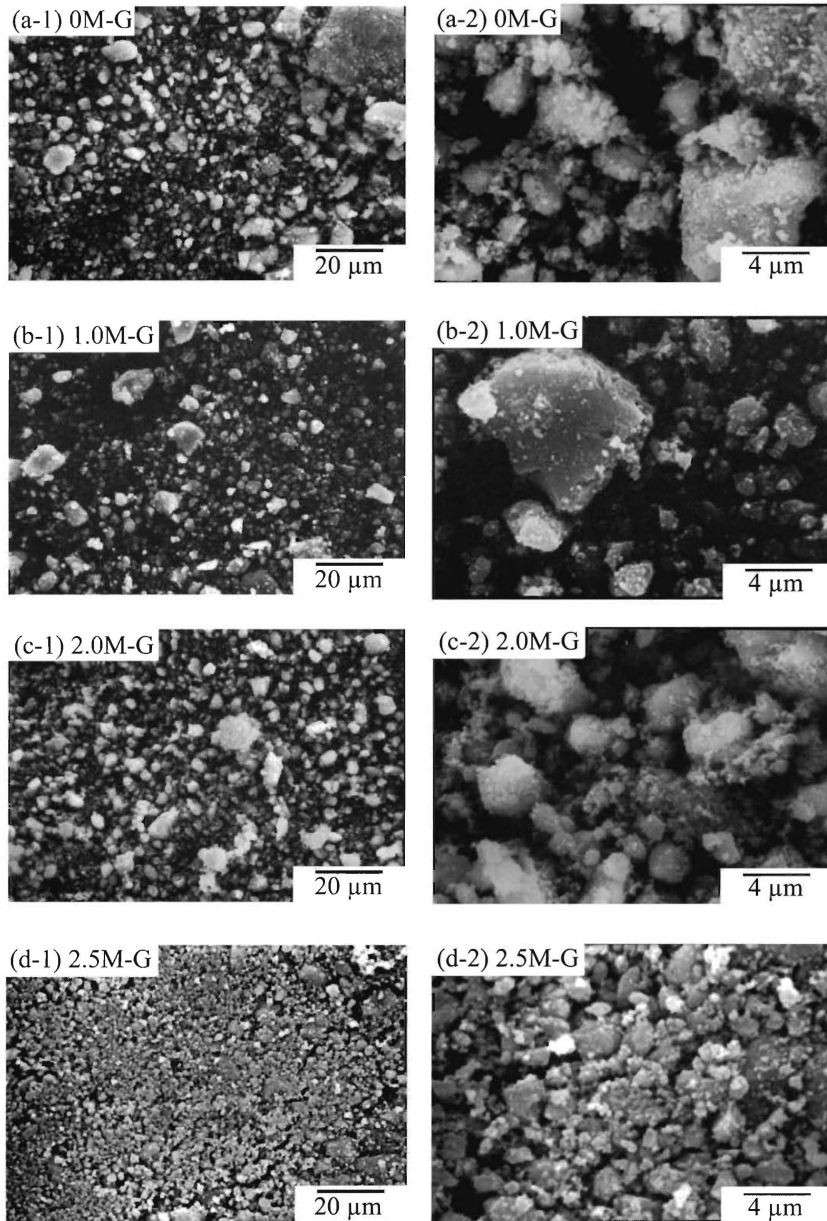


Fig. 3. SEM photographs of ground  $m\text{-SnO}_2$  powders prepared at various molar ratios of MES/SS. The powders were not subjected to UT.

From these results, it was confirmed that MES addition was ineffective in reducing the size of  $m\text{-SnO}_2$  agglomerates. On the other hand, MG after the powder preparation was effective in reducing the size of agglomerated particles, but also led to decreases in both pore volume and SSA. Therefore, the size control of secondary particles was further attempted by different treatments during the preparation of  $m\text{-SnO}_2$  powders in solution, as described in the next section.

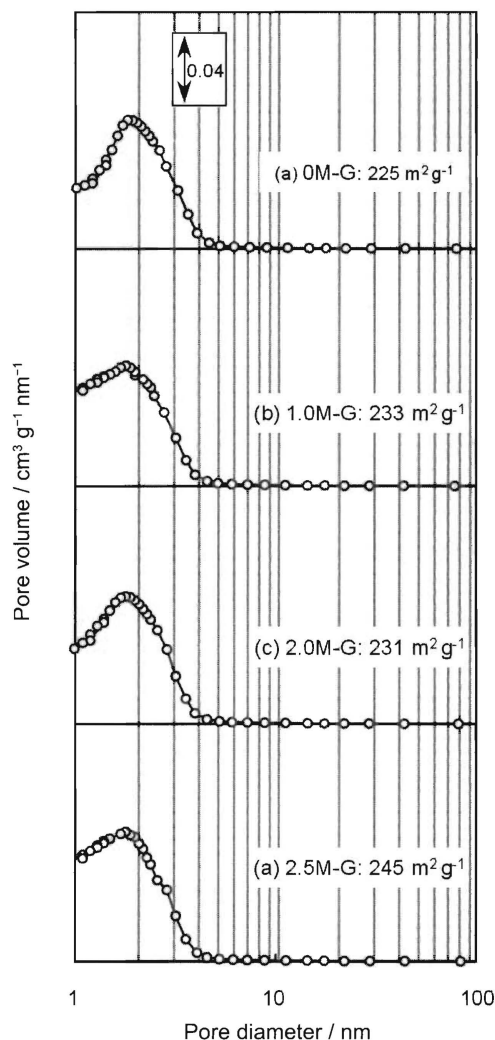


Fig. 4. Pore size distributions of ground  $m\text{-SnO}_2$  powders prepared at various molar ratios of MES/SS after grinding. The powders were not subjected to UT.

### 3.2 Effects of stirring and ultrasonic treatment

Reduction of the size of  $m\text{-SnO}_2$  agglomerates was attempted by stirring the aqueous precursor solution, thus dispersing  $m\text{-SnO}_2$  powder prepared at  $[\text{MES}]/[\text{SS}] = 2.5$  during the aging treatment for 12 h. Figure 5 shows SEM photographs of the as-prepared and ground  $m\text{-SnO}_2$  powders prepared with stirring. The size of agglomerated  $m\text{-SnO}_2$  powder was not affected markedly by stirring (compare data between 2.5M-S in Fig. 5 and 2.5M in Fig. 1) nor by the subsequent MG (compare data between 2.5M-S and 2.5M-S-G). Figure 6 shows the pore size distributions of the as-prepared and ground  $m\text{-SnO}_2$  powders prepared with stirring during aging along with their SSAs. The stirring treatment reduced both pore volume and SSA (compare data between 2.5M-S in Fig. 6 and 2.5M in Fig. 2), and the subsequent MG further reduced both pore volume and SSA; approximately 37% reduction in SSA. Therefore, the stirring treatment during the aging

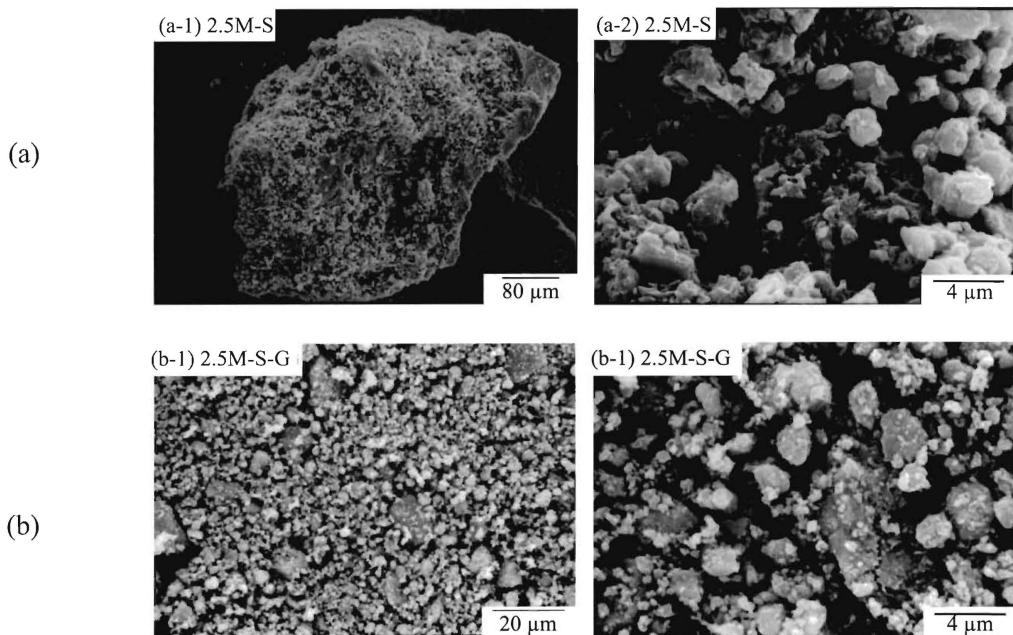


Fig. 5. SEM photographs of  $m\text{-SnO}_2$  powders prepared with stirring during aging. (a) Before and (b) after MG.

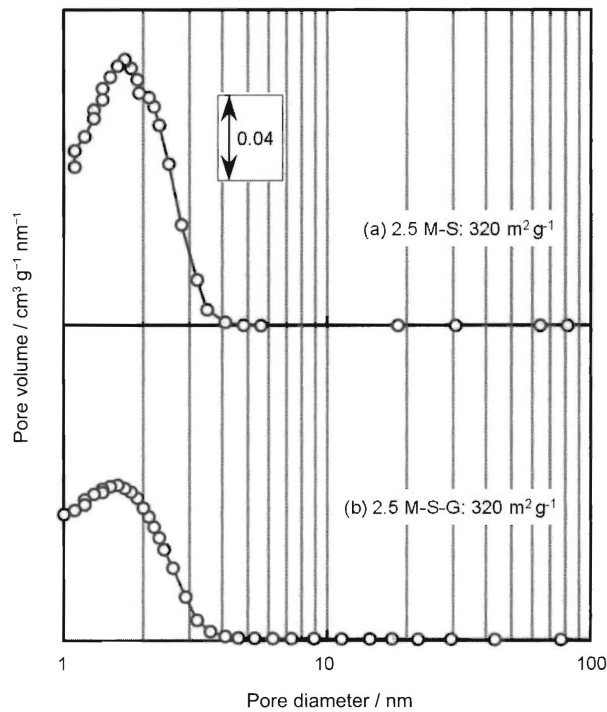


Fig. 6. Pore size distributions of  $m\text{-SnO}_2$  powders prepared with stirring during aging. (a) Before and (b) after MG.

was ineffective in maintaining the well-developed mesoporous structure as well as in reducing the size of m-SnO<sub>2</sub> agglomerates.

Next, the effect of UT on the morphology of resultant m-SnO<sub>2</sub> particles was examined. Figure 7 shows SEM photographs of the as-prepared and ground m-SnO<sub>2</sub> powders prepared with UT before aging. Among the several methods tested in this study, UT was found to be the most effective in reducing the size of as-prepared m-SnO<sub>2</sub> particles. In this case, therefore, the size of secondary particles was not affected by the subsequent MG. The SSA of 2.5M-U was almost comparable to that of 2.5M and was not reduced markedly by the subsequent MG (compare data between 2.5M-U and 2.5M-U-G), i.e., only approximately a 16% reduction, as shown in Fig. 8. Most of the mechanically brittle mesopores in m-SnO<sub>2</sub> particles might have been collapsed by UT.

### 3.3 H<sub>2</sub> sensing properties of m-SnO<sub>2</sub>

Figure 9(a) shows the operating temperature dependence of the response to 1000 ppm H<sub>2</sub> of several sensors fabricated with m-SnO<sub>2</sub> powders. Four types of m-SnO<sub>2</sub> sensors fabricated with the powders prepared at various molar ratios of [MES]/[SS] showed almost the same maximum response of 10–20 at 400 or 450°C. MG was not effective at all in improving the sensing properties, as confirmed by the comparison between 2.5M and 2.5M-G sensors, probably owing to a decrease in SAA of the powder. Among the sensors tested, it was found that the 2.5M-U sensor showed the largest H<sub>2</sub> response (approximately 80 at 400°C). Small agglomerates of micron size

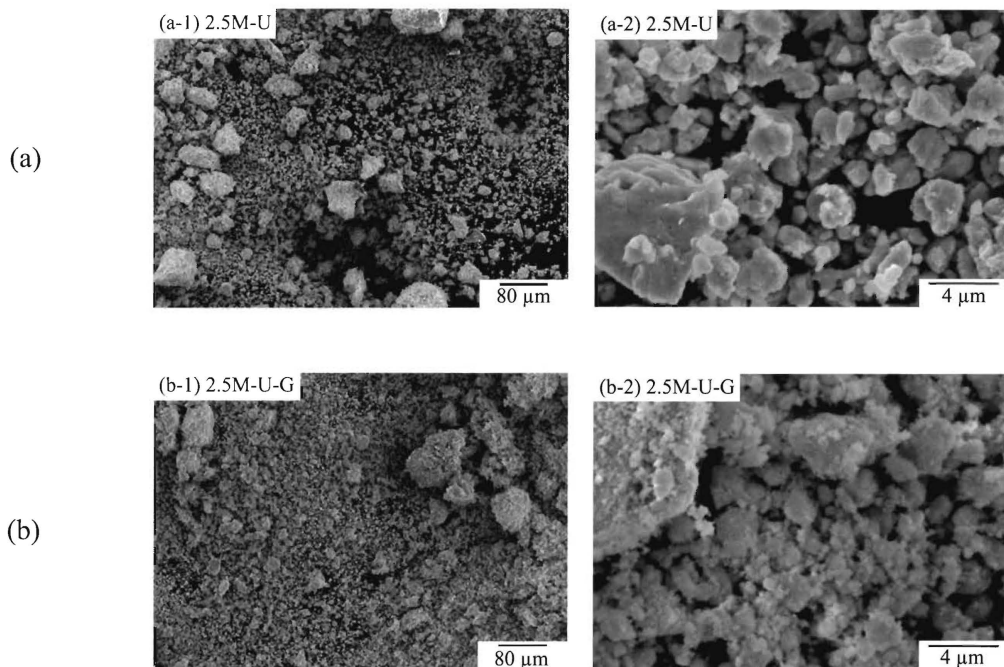


Fig. 7. SEM photographs of m-SnO<sub>2</sub> powders prepared with UT before aging. (a) Before and (b) after MG.

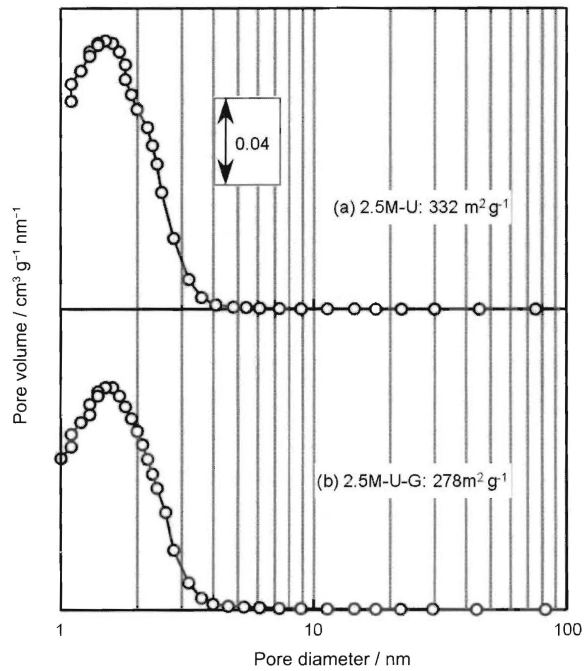


Fig. 8. Pore size distributions of  $\text{m-SnO}_2$  powders prepared with UT before aging. (a) Before and (b) after MG.

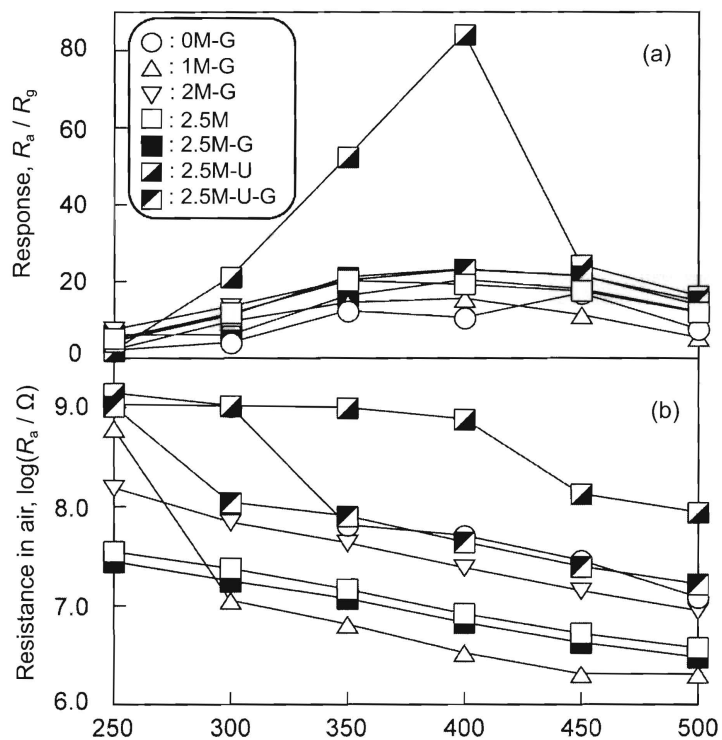


Fig. 9. Operating temperature dependence of (a) response to 1000 ppm  $\text{H}_2$  and (b) resistance in air of several  $\text{m-SnO}_2$  sensors.

observed for 2.5M-U powder with a large SSA are considered to be responsible for the largest response. Again, MG of the as-prepared powder resulted in a decrease in the H<sub>2</sub> response of the sensor from 80 to approximately 20 at 400°C. Figure 9(b) shows the operating temperature dependence of sensor resistance in air. The resistance of the 2.5M-U sensor was much higher than those of the other sensors, particularly at 350 and 400°C. The high resistance of the 2.5M-U sensor is ascribed to a large amount of chemisorbed oxygen in air owing to the large SSA as well as a large amount of some residual phosphate-related compounds existing on particle surfaces after the treatment in an aqueous phosphoric acid solution. These results show that among the methods tested, UT is the most effective in improving the H<sub>2</sub> gas sensing properties of m-SnO<sub>2</sub>.

#### 4. Conclusions

The control of molar ratios of [MES]/[SS] in the precursor solution and stirring during aging were not effective for reducing the size of m-SnO<sub>2</sub> agglomerates. The agglomerate size of m-SnO<sub>2</sub> could be reduced satisfactorily by UT before aging. In addition, a large SSA (more than 300 m<sup>2</sup> g<sup>-1</sup>) with a well-developed porous structure could be maintained by UT. MG also reduced the size of m-SnO<sub>2</sub> agglomerates, but their SSA was also reduced owing to partial destruction of the mesoporous structure. Among the m-SnO<sub>2</sub> sensors examined, the 2.5M-U sensor, which was fabricated with the m-SnO<sub>2</sub> powder subjected to UT but not to MG, showed the largest H<sub>2</sub> response (approximately 80 at 400°C), probably owing to the large SSA and small m-SnO<sub>2</sub> agglomerates.

#### References

- 1 T. Seiyama, A. Kato and K. Moriya: *Anal. Chem.* **34** (1962) 1502.
- 2 D. H. Kim, S. H. Lee and K.-H. Kim: *Sens. Actuators, B* **77** (2001) 427.
- 3 A. Hagemeyer, Z. Hogan, M. Schlichter, B. Smaka, G. Streukens, H. Turner, A. Volpe Jr., H. Weinberg and K. Yaccato: *Appl. Catal. A* **317** (2007) 139.
- 4 J.-H. Smatt, N. Schuwer, M. Jarn, W. Lindner and M. Linden: *Microporous Mesoporous Mater.* (in press).
- 5 M. E. Franke, T. J. Koplín and U. Simon: *Nanoparticles in Sens. Tech.* **2** (2006) 36.
- 6 X.-J. Huang and Y.-K. Choi: *Sens. Actuators, B* **122** (2007) 23.
- 7 D. C. Meier and S. Semancik: *Appl. Phys. Lett.* **91** (2007) 063118.
- 8 M. Vilaseca, J. Coronas, A. Cirera, A. Cornet, J. R. Morante and J. Santamaria: *Sens. Actuators, B* **124** (2007) 99.
- 9 N. Ramgir, Y. Hwang, S. Jhung, H.-K. Kim, J.-S. Hwang, I. Mulla and J.-S. Chang: *Surf. Sci.* **252** (2006) 4298.
- 10 C. Ge, C. Zie, M. Hu, Y. Gui, Z. Bai and D. Zeng: *Mater. Sci. Eng. B* **141** (2007) 43.
- 11 S. Choopun, N. Hongsith, P. Mangkorntong and N. Mangkorntong: *Physica E* **29** (2007) 53.
- 12 J. Van, A. Lassesson, S. A. Brown, M. Schulze, J. G. Partridge and A. Ayes: *Appl. Phys. Lett.* **91** (2007) 181910.
- 13 T. Hyodo, S. Abe, Y. Shimizu and M. Egashira: *Sens. Actuators, B* **93** (2003) 590.
- 14 Y. Shimizu, A. Jono, T. Hyodo and M. Egashira: *Sens. Actuators, B* **108** (2005) 56.